

Supporting Information:

NMRlipids IV: Headgroup & glycerol backbone structures, and cation binding in bilayers with PE and PG lipids

Pavel Buslaev,[†] Rebeca García Fandiño,[¶] Fernando Favela-Rosales,^{||} Tiago Ferreira,[⊥] Patrick Fuchs,[#] Ivan Gushchin,[‡] Matti Javanainen,[@] Anne M. Kiirikki,[△] Jesper J. Madsen,^{∇,††} Josef Melcr,^{@,‡‡} Paula Milan Rodriguez,[#] Markus S. Miettinen,^{¶¶} O. H. Samuli Ollila,^{*,△} Chris G. Papadopoulos,^{§§} Antonio Peón,^{|||} Thomas J. Piggot,^{⊥⊥} and Ángel Piñeiro^{##}

[†]*Nanoscience Center and Department of Chemistry, University of Jyväskylä, Finland*

[‡]*Research Center for Molecular Mechanisms of Aging and Age-related Diseases, Moscow Institute of Physics and Technology, Dolgoprudny, Russia*

[¶]*Center for Research in Biological Chemistry and Molecular Materials (CiQUS), Universidade de Santiago de Compostela, E-15782 Santiago de Compostela, Spain*

[§]*CIQUP, Centro de Investigaçãõ em Quãmica, Departamento de Quãmica e Bioquãmica, Faculdade de Ciãncias, Universidade do Porto, Porto, Portugal*

^{||}*Departamento de Ciencias Básicas, Tecnológico Nacional de México, Campus Zacatecas Occidente, México*

[⊥]*Halle, Germany*

[#]*Paris, France*

[@]*Institute of Organic Chemistry and Biochemistry of the Czech Academy of Sciences, Flemingovo nám. 542/2, CZ-16610 Prague 6, Czech Republic*

[△]*Institute of Biotechnology, University of Helsinki*

[∇]*Department of Chemistry, The University of Chicago, Chicago, Illinois, United States of America*

^{††}*Department of Global Health, College of Public Health, University of South Florida, Tampa, Florida, United States of America*

^{‡‡}*Groningen Biomolecular Sciences and Biotechnology Institute and The Zernike Institute for Advanced Materials, University of Groningen, 9747 AG Groningen, The Netherlands*

^{¶¶}*Department of Theory and Bio-Systems, Max Planck Institute of Colloids and Interfaces, 14424 Potsdam, Germany*

^{§§}*I2BC - University Paris Sud*

^{|||}*Spain*

^{⊥⊥}*Chemistry, University of Southampton, Highfield, Southampton SO17 1BJ, United Kingdom*

^{##}*Departamento de Física Aplicada, Faculdade de Física, Universidade de Santiago de Compostela, E-15782 Santiago de Compostela, Spain*

E-mail: samuli.ollila@helsinki.fi

Contents

S1 R-PDLF and SDROSS experiments	S3
S2 Lipid ligand names in PDB used in the analysis of conformations of protein-bound lipids	S6
S3 Evaluation of simulations against NMR experiments	S7
S3.1 Conformational ensembles of headgroup and glycerol backbone in PE and PG lipids	S7
S3.2 PC headgroup in mixtures with PE or PG lipids	S10
S3.3 PG headgroup in mixtures with PC lipids	S12
S3.4 Calcium binding to POPC:POPG mixtures	S13
S4 Dihedral angle distributions and the analysis of relative energies	S18
S5 Changes in headgroup conformations upon addition of charged surfactants or CaCl₂	S19
S6 Simulated systems	S22
S6.1 CHARMM36	S23
S6.2 CHARMM36ua	S23
S6.3 Slipids	S24
S6.4 Berger	S25
S6.5 GROMOS 43A1-S3	S25
S6.6 OPLS-UA	S25
S6.7 GROMOS-CKP and GROMOS-CKPM	S26
S6.8 OPLS-MacRog	S26
S6.9 Lipid17	S26
S6.10Lipid17ecc	S27

S1 R-PDLF and SDROSS experiments

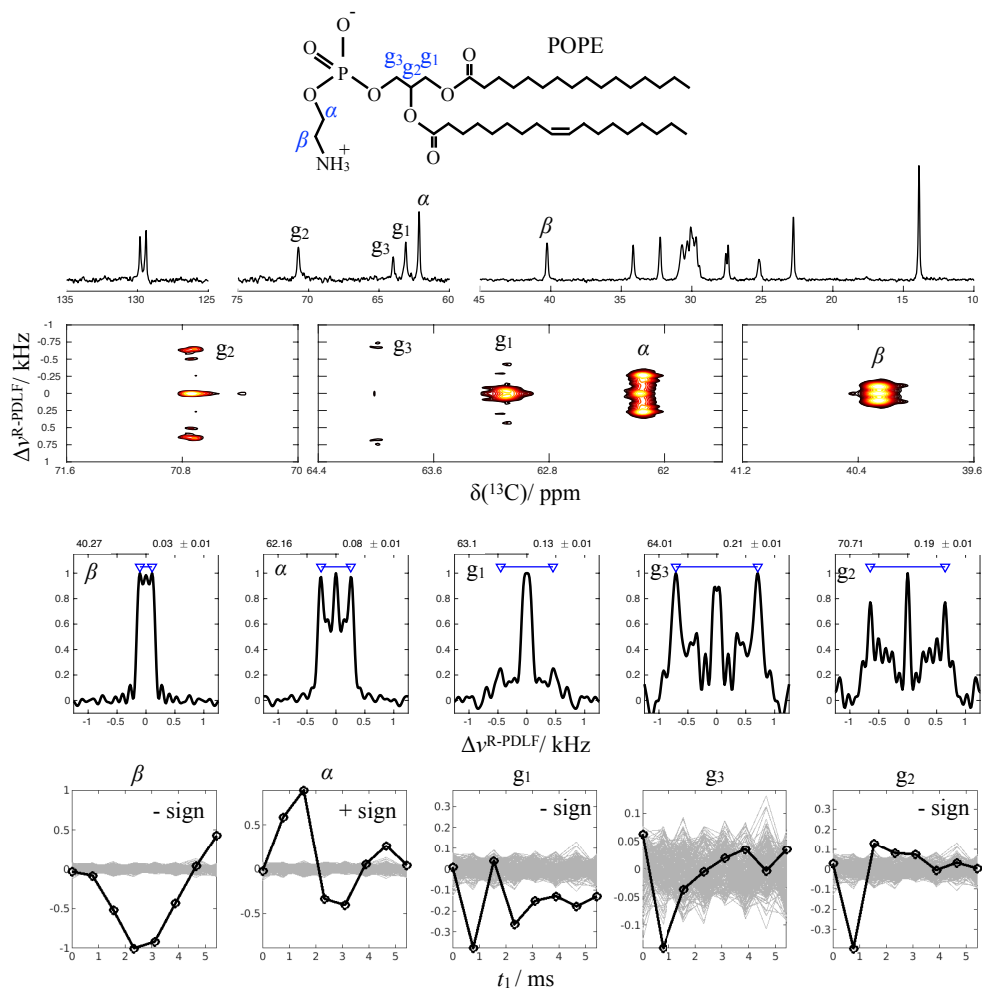


Figure S1: (A) Chemical structure of POPE with the labeling of headgroup and glycerol backbone carbons. (B) INEPT spectra from POPE sample with the headgroup and glycerol backbone peaks labeled. (C) 2D R-PDLF spectra (D) Dipolar slices from the 2D R-PDLF spectra with the resulting order parameters on top of figures. (E) Experimental S-DROSS curves giving signs of the order parameters.

1.A, B etc. labels to be put in the figure.



Figure S2: (A) Chemical structure of POPG with the labeling of headgroup and glycerol backbone carbons. (B) INEPT spectra from POPG sample with the headgroup and glycerol backbone peaks labeled. (C) 2D R-PDLF spectra (D) Dipolar sliced from the 2D R-PDLF spectra with the resulting order parameters on top of figures. (E) Experimental S-DROSS curves giving signs of the order parameters.

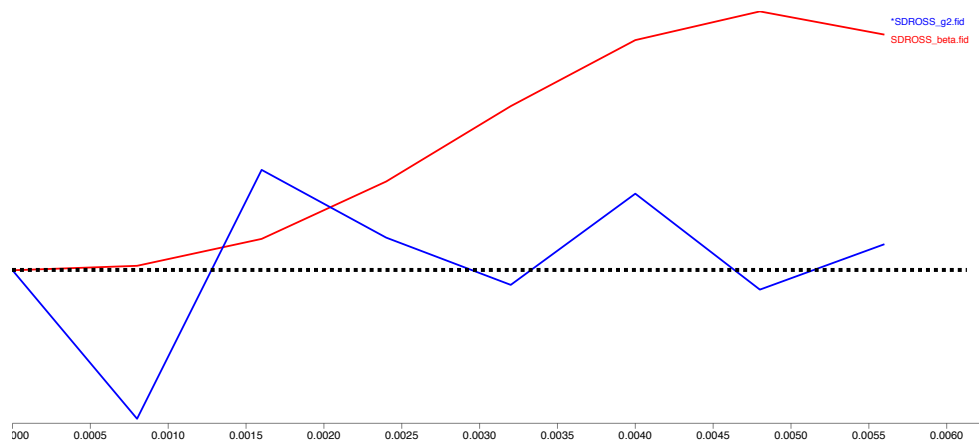


Figure S3: Simpson simlaton of S-DROSS curve of β -carbon of POPG.

S2 Lipid ligand names in PDB used in the analysis of conformations of protein-bound lipids

PC: PLC, PX4, 6PL, LIO, HGX, PC7, PC8, P1O, 6O8, XP5, EGY, PLD, SBM, HXG, and PCW

PE: 8PE, PTY, 3PE, PEH, PEF, 6OE, 6O9, 9PE, PEV, 46E, SBJ, L9Q, PEK, EPH, ZPE, 9TL, 9Y0, 6OU, LOP, and PEE

PG: PGT, PGK, LHG, 44G, PGV, OZ2, D3D, PGW, DR9, P6L, PG8, H3T, and GOT

PS: PSF, PS6, Q3G, P5S, D39, PS2, 17F, and 8SP.

S3 Evaluation of simulations against NMR experiments

S3.1 Conformational ensembles of headgroup and glycerol backbone in PE and PG lipids

The quality of PE and PG headgroup conformational ensembles in different simulations against NMR experiments is evaluated in figures S4 and S5 using C-H bond order parameters as in our previous studies for PC and PS lipids.^{1,2} Conclusions are the same for all lipids: None of the force fields correctly captures the lipid headgroup conformational ensembles, but CHARMM36 gives results closest to experiments.

It should be noted that the PG headgroup is biologically abundant R enantiomer in all simulations, while our ^{13}C NMR experiments has a racemic mixture. Nevertheless, previous ^2H NMR experiments comparing results between different enantiomers concluded that the structural differences between these are minor.³

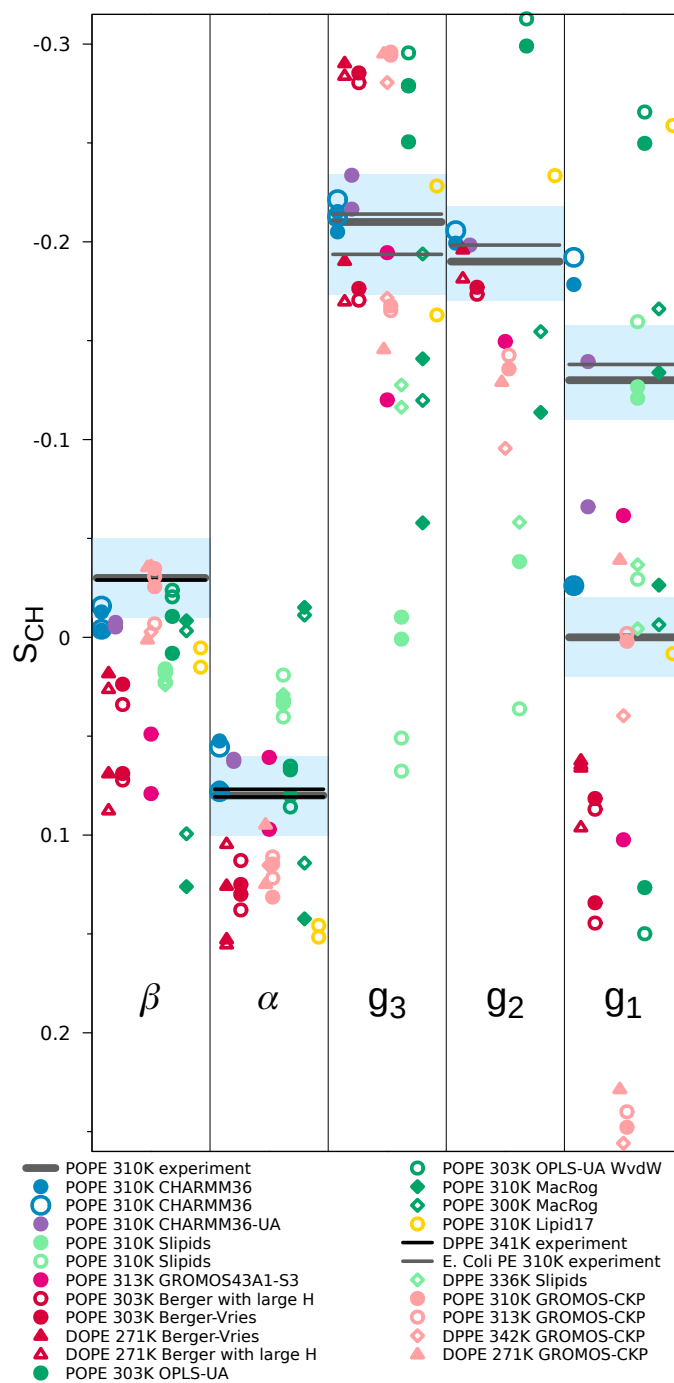


Figure S4: The headgroup and glycerol backbone order parameters of PE lipids from experiments (POPE and signs this work, DPPE from Ref. 4 and E.coliPE from Ref. 5) and simulations with different force fields.

2.This should be clarified as in NMRlipidsI and error bars should be added. Probably larger error bars for united atom models based on the report by Fuchs et al.

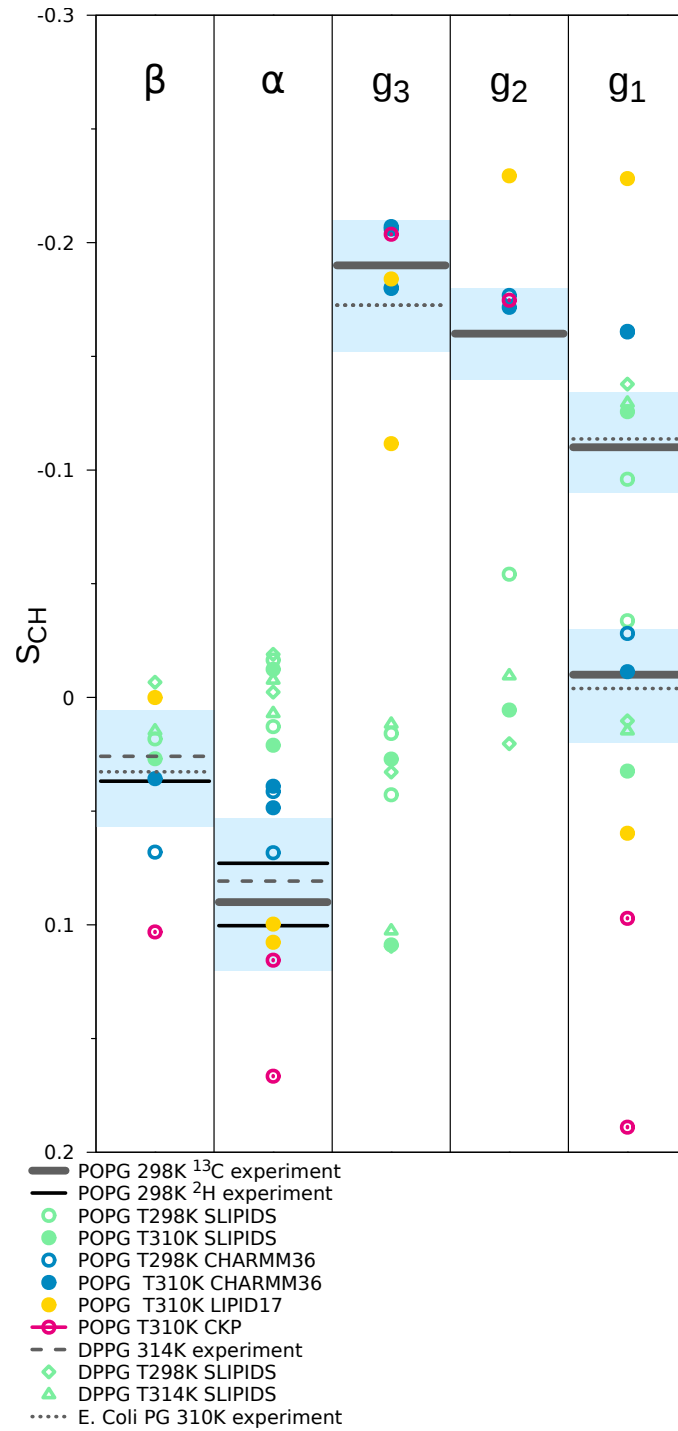


Figure S5: The headgroup and glycerol backbone order parameters of PG lipids from experiments (POPG and signs from this work and from Ref. 6, DPPG with 100mM NaCl from Ref. 3, and E. Coli PG results from Ref. 5) and simulations with different force fields.

S3.2 PC headgroup in mixtures with PE or PG lipids

Headgroup order parameters of PC lipids are unchanged upon addition of zwitterionic lipids or cholesterol in experiments, but increase upon addition of negatively charged PG or PS lipids because headgroup dipole tilts more parallel to the membrane plane after incorporation of negative charges into the membrane.^{7,10,11} The response of PC headgroup order parameters to the addition of PE or PG lipids from different simulations is compared with experiments in figure S6. None of the simulations reproduce neither the experimentally observed increase in PC headgroup order parameters with increasing amount of PG nor the related tilting of the headgroup more parallel with the membrane. Similar observations in our previous work for PS lipids were explained by the overestimated counterion binding affinity that neutralizes the effect of added negative charge.² All simulations except Berger-OPLS predict tilting of P-N headgroup outwards from the membrane and decrease of PC headgroup order parameters upon addition of PE lipids. These results are not in line with experiments where the PC headgroup order parameters are not affected by zwitterionic lipids.⁷ The good performance of Berger-OPLS simulations in here is surprising because headgroup conformational ensemble is not very close to experiments in this model and the response of headgroup order parameters to cholesterol was significantly overestimated by the Berger/Höltje force field in our previous work.¹

In conclusion, more accurate force fields are needed to correctly simulate the interactions between different headgroups.



Figure S6: Modulation of POPC headgroup order parameters with increasing amount of POPE (left) and POPG (right) in bilayer from experiments at 298 K^{7,8} and simulations with different force fields (temperatures listed in tables S3 and S4 are between 298-310 K). Signs are determined as discussed in Refs. 1,9.

S3.3 PG headgroup in mixtures with PC lipids

Changes in other than PC lipid headgroup with changing membrane composition are less extensively characterized in the literature. The β -carbon order parameter in PG headgroup increases mildly⁸ or is unchanged⁶ upon increasing amount of PC lipids (Fig. S7), but experimental data from α -carbon is not available. Also the tested force fields predict very small changes for the β -carbon order parameter, while the P-N vector tilt and its response to the increased amount of PC varies significantly between force fields in figure S7. Therefore, more experimental data and more accurate force fields are still required to resolve the PG conformational ensembles in mixtures with other lipids.



Figure S7: Modulation of PG lipid headgroup order parameters with the increasing amount of PC in lipid bilayer from experiments at 298 K^{6,8} and simulations with different force fields at 310 K.

S3.4 Calcium binding to POPC:POPG mixtures

The changes of headgroup order parameters in POPC:POPG mixtures upon addition of CaCl_2 between different simulations and experiments^{6,8} are compared in figures S8 (molar ratio 1:1) and S10 (molar ratio 4:1). The results are in line with our previous studies: most force fields overestimate the calcium binding,^{2,12} but CHARMM36 with the NBfix correction underestimates the binding affinity,² and the implicit inclusion of electronic polarizability using the electronic continuum correction (ECC) improves the results.^{13,14}

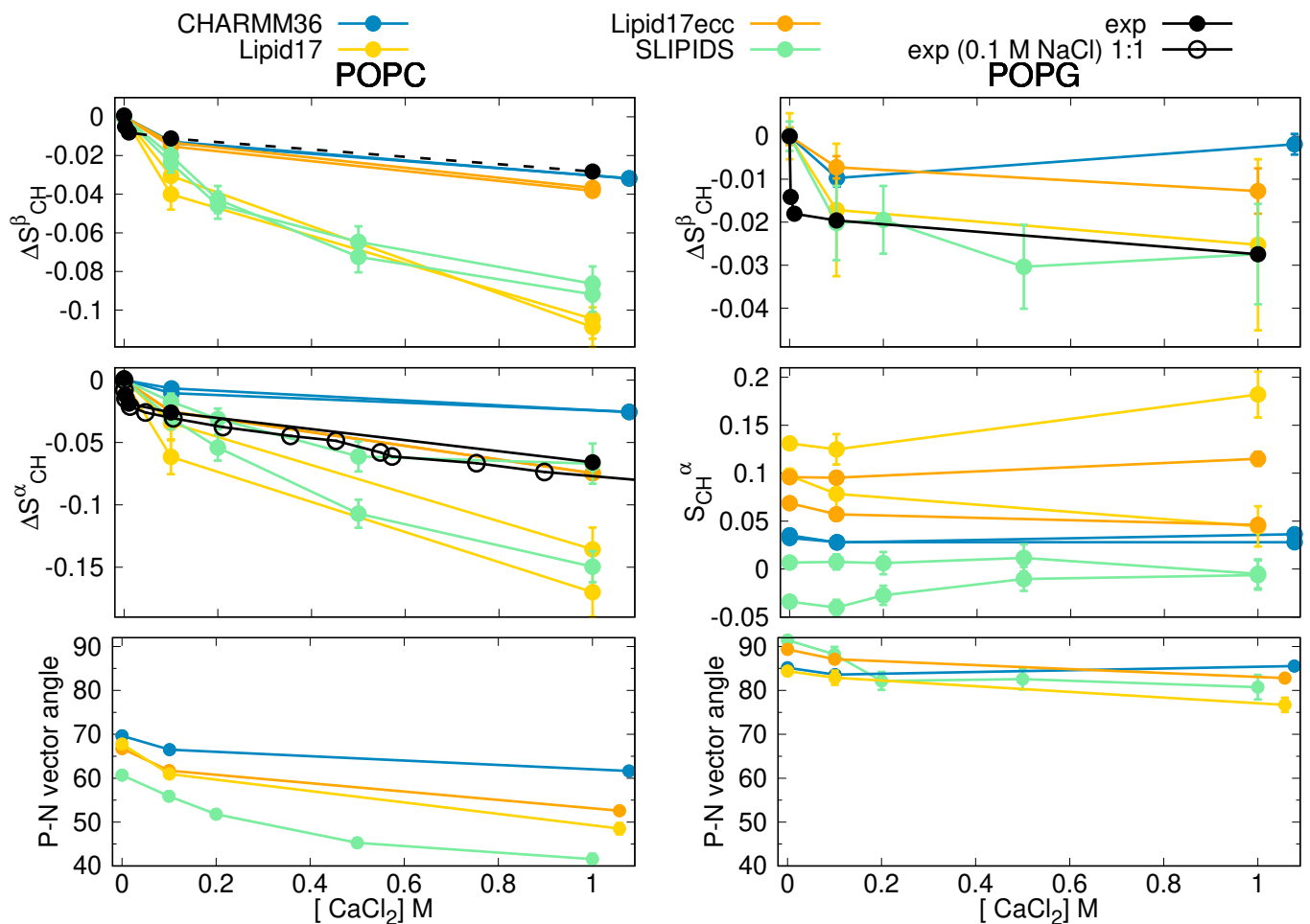


Figure S8: Modulation of headgroup order parameters of POPC (*left*) and POPG (*right*) in POPC:POPG (1:1) mixture upon addition of CaCl_2 in 298 K temperature from experiments^{6,8} and simulations. The β -carbon order parameter of POPC (dashed line on top left) is not directly measured but calculated from empirical relation $\Delta S_\beta = 0.43\Delta S_\alpha$.¹⁵ The changes with respect to the systems without CaCl_2 are shown for other data than for the α -carbon of POPG for which experimental order parameter is not available. Calcium density distributions are shown in figure S9.

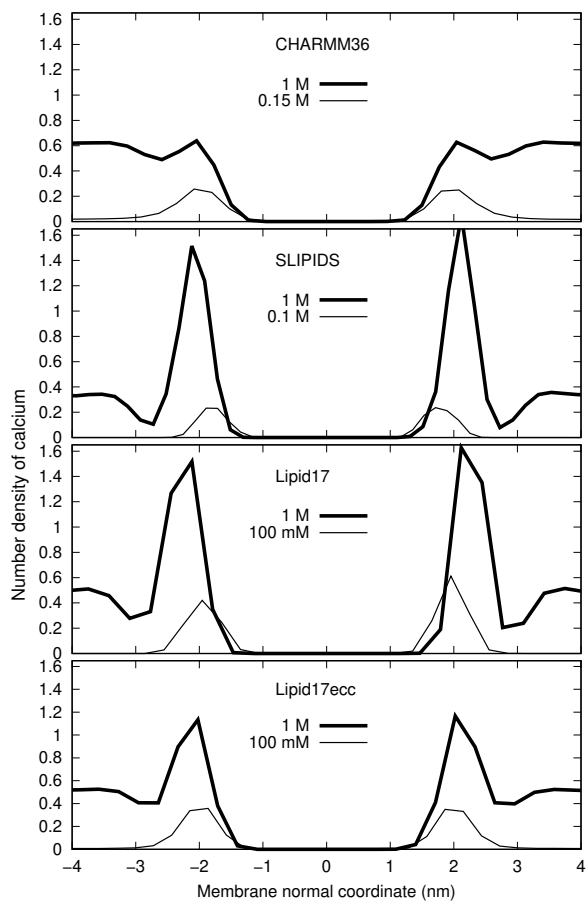
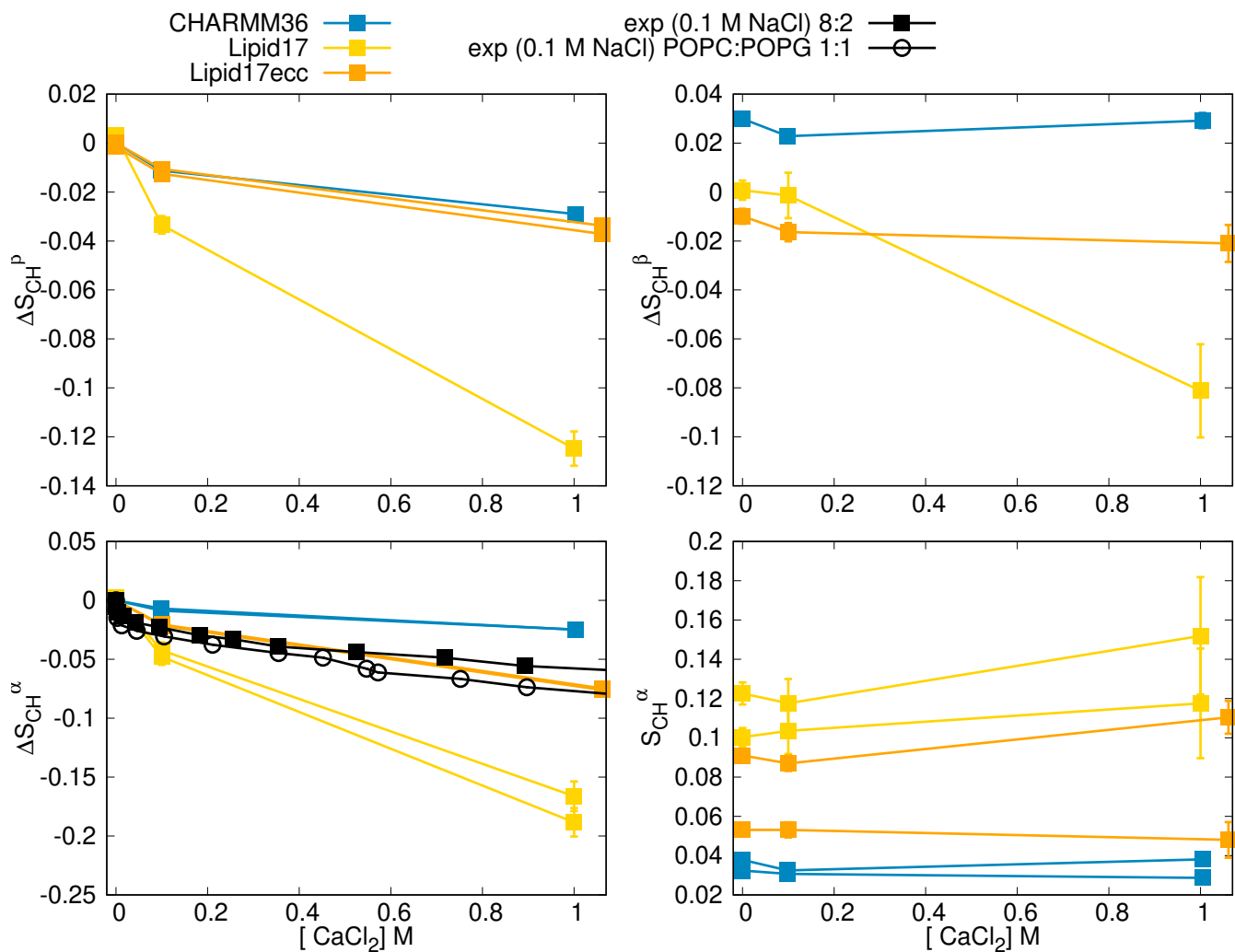


Figure S9: Calcium ion density profiles along membrane normal from simulations of POPC:POPG (1:1) mixtures with different force fields. The changes in the order parameters upon addition of CaCl_2 are compared with experiments in figure S8.



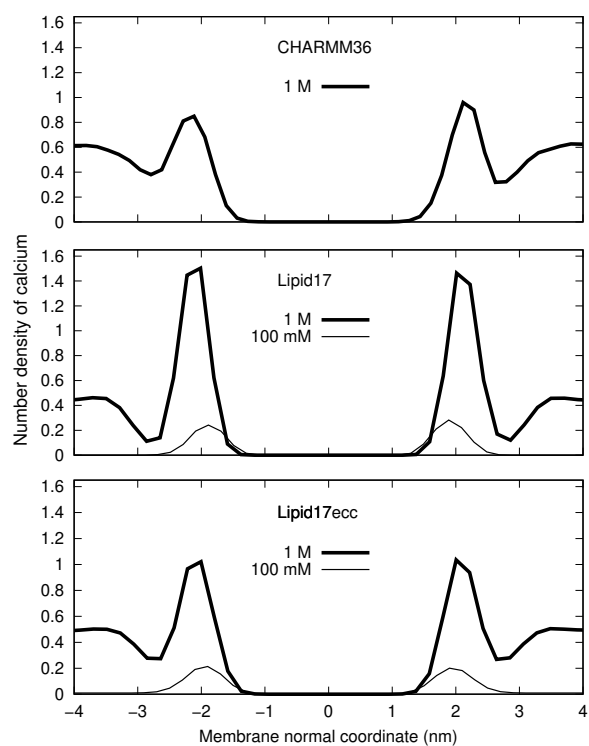


Figure S11: Calcium ion density profiles along membrane normal from simulations of POPC:POPG (4:1) mixtures with different force fields.

S4 Dihedral angle distributions and the analysis of relative energies

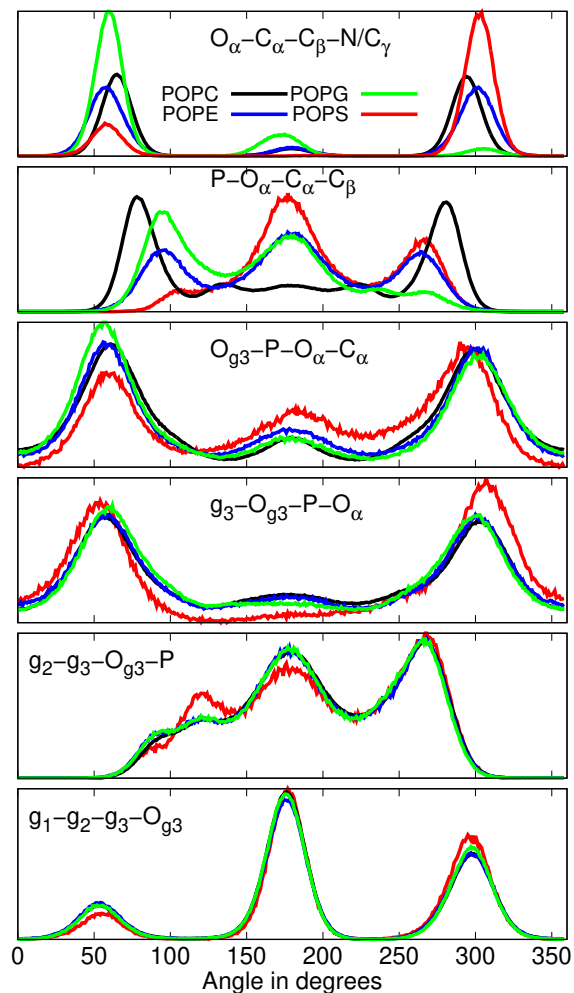


Figure S12: Heavy atom dihedral angle distributions from CHARMM36 simulations that correctly capture the order parameter differences between the force fields.

S5 Changes in headgroup conformations upon addition of charged surfactants or CaCl_2

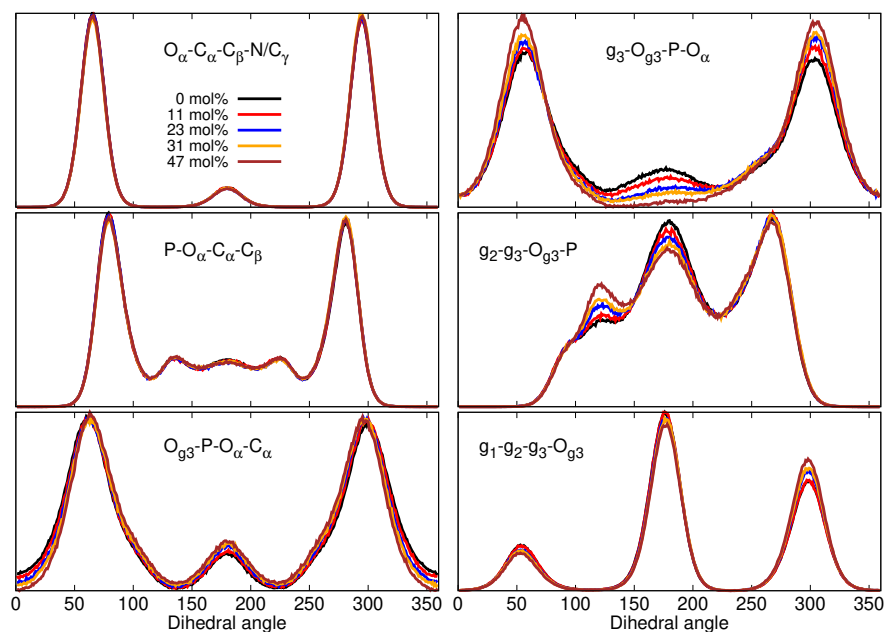


Figure S13: Changes in PC headgroup conformational ensembles upon increasing the amount of positive charge in bilayer, characterized by the heavy atom dihedral distributions, from CHARMM36 simulations.



Figure S14: Changes in POPC lipid17ecc dihedrals with increasing amount of CaCl_2 .



Figure S15: Changes in POPC CHARMM36 dihedrals with increasing amount of CaCl_2 .

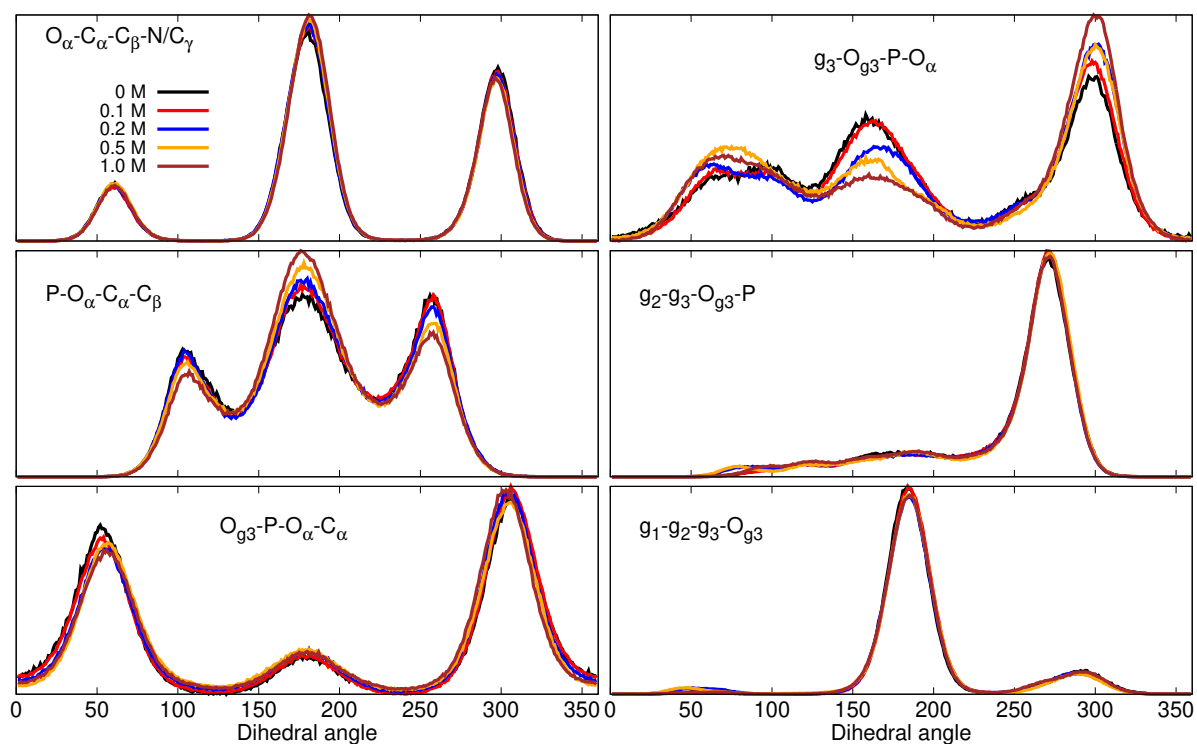


Figure S16: Changes in POPG Slipids dihedrals with increasing amount of CaCl_2 .

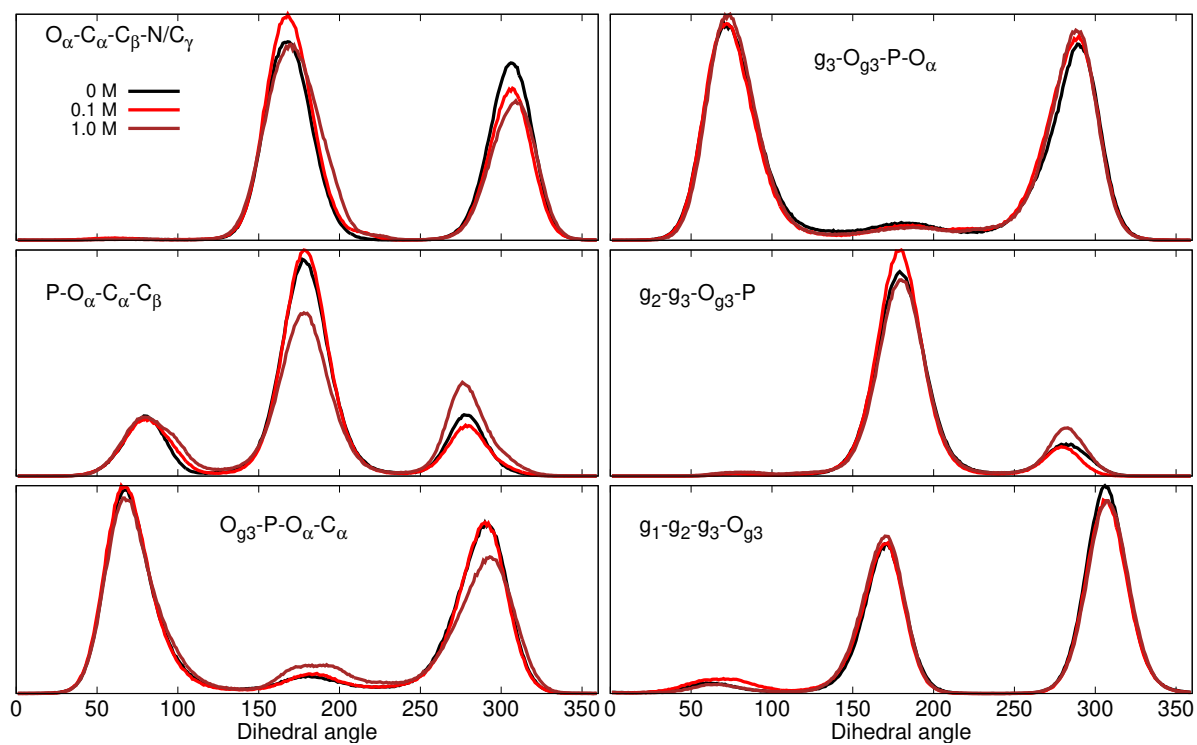


Figure S17: Changes in POPG lipid17 dihedrals with increasing amount of CaCl_2 .

S6 Simulated systems

The simulated systems of pure PE and PG bilayers without additional ions are listed in Tables S1 and S2, and lipid mixtures with additional ions in Tables S3 and S4. The simulations were analyzed using preliminary versions of the NMRLipids databank (www.nmrlipids.fi, github.com/NMRLipids/MATCH and <https://github.com/NMRLipids/NMRLipidsIVPEandPG/tree/master/Data/Simulations>) and unique naming convention for lipid atoms (<http://nmrlipids.blogspot.com/2015/03/mapping-scheme-for-lipid-atom-names-for.html>), which enable automatic analysis of simulations with different force fields with varying atom naming conventions. The automatic analyses were implemented using MDAnalysis^{16,17} and MDTraj¹⁸ python libraries, and tools in the GROMACS software package.¹⁹ All codes are available from the project’s GitHub repository.²⁰

The C–H bond order parameters were calculated directly from the carbon and hydrogen positions using the definition

$$S_{\text{CH}} = \frac{1}{2} \langle 3 \cos^2 \theta - 1 \rangle, \quad (1)$$

where θ is the angle between the C–H bond and the membrane normal (taken to align with z , with bilayer periodicity in the xy -plane). Angular brackets denote average over all sampled configurations. The order parameters were first calculated averaging over time separately for each lipid in the system. The average and the standard error of the mean were then calculated over different lipids. Code for all atom simulations is available in Ref. 21 (`scripts/calcOrderParameters.py`). For united atom simulations, we first constructed trajectories including hydrogens with ideal geometry using either `buildH` program²² or (`scratch/opAAUA_prod.py`) in Ref. 21, and the order parameters were then calculated from these trajectories. This approach has been tested against trajectories with explicit hydrogens and the deviations in order parameters are small.^{22,23}

S6.1 CHARMM36

POPE **17.Simulation details by M. Javanainen.**

POPE with additional NaCl **18.Simulation details by A. Peon.**

POPG Lipid bilayer containing 118 POPG molecules, 4110 TIP3P water molecules, and 118 potassium ions was build using CHARMM-GUI.¹⁰⁹ The system was simulated 100 ns, coupled to 298 K using Nose-Hoover^{110,111} thermostat and 1 bar with semi-isotropic Parrinello-Rahman¹¹² pressure coupling. The used default parameters and force field files from CHARMM-GUI were used. The used files are available from 54.

19.Simulation details for larger simulation by A. Peon.

POPG with additional NaCl **20.Simulation details by A. Peon.**

POPC:POPE mixtures Data is available at.^{77,78} 300 K with v-rescale ($\tau=0.1$ ps), 1 bar with PR semiisotropic ($\tau=4$ ps, compressibility= $4.5\text{e-}5$ bar⁻¹), PME order 4 and space 0.12, rcoulomb and rvdw 1.0, 128 lipids per leaflet, no ion **21.Full simulation details by Fuchs et al.**

POPC:POPG 1:1 and POPC:POPG 4:1 mixtures with additional calcium The initial structures were built with CHARMM-GUI Membrane Builder.¹⁰⁹ The TIP3P water model was used to solvate the systems. The simulations were run for 400 ns with timestep 2 fs and the first 100 ns were discarded as equilibration time. The simulations were run with GROMACS version 2020.2.¹¹³ The Nose-Hoover thermostat^{110,111} was used with temperature of 298 K and the time constant for temperature coupling was 1.0 ps. The semi-isotropic Parrinello-Rahman barostat¹¹² was used with reference pressure 1.0 bar and with a time constant of 5.0 ps with compressibility of $4.5\text{e-}5$ bar⁻¹. Long range electrostatic interactions were calculated with the PME method. All bonds with hydrogen atoms were constrained with LINCS algorithm. The simulation files are available from Refs. 71–76.

POPC and POPC:POPG (7:3) mixture **22.Simulation details by A. Peon.**

S6.2 CHARMM36ua

POPE Data is available at.²⁸ **23.Simulation details by T. Piggot.**

S6.3 Slipids

POPE Data is available at.³¹ **24.Simulation details by T. Piggot.**

POPE with additional NaCl **25.Simulation details by A. Peon. I have assumed that ion parameters are default Slipids, i.e., Åqvist, please correct if this is not true.**

DPPE with 288 lipids. The starting structure for simulation with 288 DPPE lipids and 9386 water molecules was constructed with the MEMBRANE BUILDER website.¹¹⁴ The TIP3P¹¹⁵ water model was used to solvate the system. Simulation was performed for 200 ns, and the last 100 ns were used for the analysis. Simulation was carried out within the NPT ensemble using the GROMACS 5.0.4 package.¹¹⁶ Timestep of 2 fs was used with the leapfrog integrator. The Nosé–Hoover thermostat^{110,111} was used with reference temperature of 336 K and a relaxation time constant of 0.5 ps; lipids and water were coupled separately to the heat bath. Pressure was kept constant at 1.013 bar using a semi-isotropic Parrinello–Rahman barostat¹¹² with a time constant of 10.0 ps. Long-range electrostatic interactions were calculated using the PME method.^{117,118} A real space cut-off of 1.0 nm was employed with grid spacing of 0.12 nm in the reciprocal space. Lennard-Jones potentials were cut off at 1.4 nm, with a dispersion correction applied to both energy and pressure. All covalent bonds in lipids were constrained using the LINCS algorithm,¹¹⁹ whereas water molecules were constrained using SETTLE.¹²⁰ Twin-range cutoffs, 1.0 nm and 1.6 nm, were used for the neighbor lists with the long-range neighbor list updated every 10 steps.

POPG with 288 lipids. The starting structure for simulation with 288 POPG lipids, 10664 water molecules and 288 Na ions was constructed with the MEMBRANE BUILDER website.¹¹⁴ The TIP3P¹¹⁵ water model was used to solvate the system and Ions are described by the parameters derived by Åqvist.³³ Simulation was performed for 250 ns, and the last 100 ns were used for the analysis. Same simulation conditions as DPPE with reference temperature of 298 K.

POPG with additional NaCl **26.Simulation details by A. Peon. I have assumed that ion parameters are default Slipids, i.e., Åqvist, please correct if this is not true.**

DPPG with 288 lipids. The starting structure for simulation with 288 DPPG lipids, 11232 water molecules and 288 Na ions was constructed with the MEMBRANE BUILDER website.¹¹⁴ The TIP3P¹¹⁵ water model was used to solvate the system and Ions are described by the parameters derived by Åqvist.³³ For the 298 K temperature, simulation was performed for 400 ns, and the last 100 ns were used for the analysis. For the 314 K temperature, simulation was performed for 200 ns, and the last 100 ns were used for the analysis. Same simulation conditions as DPPE for both temperatures.

POPC:POPG mixture with additional NaCl **27.Simulation details by A. Peon. I have assumed that ion parameters are default Slipids, i.e., Åqvist, please correct if this is not true.**

POPC:POPG mixture with additional CaCl **28.Simulation details by M. Javanainen.**

S6.4 Berger

POPE Data is available at.^{46,47} **29.Simulation details by T. Piggot.**

DOPE Data is available at.^{48,49} **30.Simulation details by T. Piggot.**

POPC:POPE, POPC:DOPE and DOPC:DOPE mixtures Data is available at.^{104,105} 300 K with v-rescale (tau=0.1 ps), 1 bar with PR semiisotropic (tau=4 ps, compressibility=4.5e-5 bar⁻¹), PME order 4 and space 0.12, rcoulomb and rvdw 1.0, 128 lipids per leaflet, no ion **31.Simulation details by Fuchs et al.**

S6.5 GROMOS 43A1-S3

POPE Data is available at.⁴⁰ **32.Simulation details by T. Piggot.**

S6.6 OPLS-UA

POPE Data is available at.⁴² **33.Simulation details by T. Piggot.**

POPE with vdW interaction in H Data is available at.⁴¹ **34.Simulation details by T. Piggot.**

S6.7 GROMOS-CKP and GROMOS-CKPM

POPE Data is available at.³⁶ **35.Simulation details by T. Piggot.**

DOPE Data is available at.³⁹ **36.Simulation details by T. Piggot.**

DPPE Data is available at.³⁵ **37.Simulation details by T. Piggot.**

POPG **38.Simulation details by A. Peon.**

POPC:POPG mixture **39.Simulation details by A. Peon.**

S6.8 OPLS-MacRog

POPE **40.Simulation details by M. Javanainen and P. Fuchs.**

POPC:POPE mixtures **41.Simulation details by P. Fuchs.**

S6.9 Lipid17

POPE **42.Simulation details by A. Peon.**

POPG **43.Simulation details by A. Peon.**

POPC:POPG 4:1 and POPC:POPG 1:1 mixtures with different CaCl₂ concentrations Initial structures were build by removing appropriate amount of lipids from POPC:POPG 7:3 mixture available from Ref. 121. Force field parameters from the same reference were used **44.We still need description from A. Peon how these were obtained**, except that incorrect dihedrals with type 1 were changed to type 9 (for details, see discussion in <https://github.com/NMRLipids/NMRLipidsIVPEandPG/issues/12>). Simulations were performed using the Gromacs simulation package¹¹³ with the time step of 2 fs. The non-bonded interactions were calculated directly within 1.0 nm cutoff; the Verlet scheme was used;¹²² and the long-range electrostatic forces were calculated using particle mesh Ewald.¹¹⁸ The bond lengths of hydrogen atoms were constrained using LINCS.¹¹⁹ Temperature was coupled to the velocity rescaling thermostat¹²³ at 298 K with a coupling constant of 1 ps. Pressure was coupled to the Parrinello–Rahman barostat¹¹² at 1 bar with a coupling constant of 10 ps. For

simulations with CaCl_2 , appropriate amount of ions with Dang^{63,64} parameters were added into the solvent. The simulation files are available from Refs. 89–94

S6.10 Lipid17ecc

POPC:POPG 4:1 and POPC:POPG 1:1 mixtures with different CaCl_2 concentrations Implicit inclusion of electronic polarizability by electronic continuum correction (ECC), implemented by scaling the partial charges in force fields, can be used to improve ion interactions with lipids and other biomolecules in classical MD simulations.¹²⁴ For Amber Lipid14/17 force fields, ECC has been previously implemented by scaling the charges and Lennard-Jones σ s of headgroup, glycerol backbone, and carbonyl regions by constant factors.^{13,14} Here, we apply similar ECC approach to Amber Lipid17 PG parameters as done previously for PS:¹⁴ charges and Lennard-Jones σ s of headgroup, glycerol backbone, and carbonyl regions of parameters POPG from Ref. 121 were scaled by factors of $f_q=0.75$ and $f_\sigma=0.89$, respectively (and the dihedral types were corrected to type 9 as in previous section). Previously introduced ECC-POPC parameters (scaling factors $f_q=0.8$ and $f_\sigma=0.89$ applied to Lipid14 POPC parameters) were used for POPC.¹³ ECC-ion parameters with the scaled charges^{95–97} from bitbucket.org/hseara/ions/src/master/, and SPC/E water model¹²⁵ were used in these simulations. Rest of the simulation parameters and initial configurations were taken from Lipid17 simulations.^{89–94} Simulation files of Lipid17ecc simulations are available from Refs. 98–103.

Table S1: List of MD simulations with PE lipids.

lipid	force field for lipids / ions	NaCl (M)	^a N _l	^b N _w	^c N _c	^d T (K)	^e t _{sim} (ns)	^f t _{anal} (ns)	^g files
POPE	CHARMM36 ²⁴	0	144	5760	0	310	500	400	²⁵
POPE	CHARMM36 ²⁴	0	500	25000	0	310	500	100	²⁶
POPE	CHARMM36 ²⁴	0.11	500	25000	50	310	500	100	²⁷
POPE	CHARMM36ua [?]	0	336	15254	0	310	2×200	2×100	²⁸
DPPE	Slipids ²⁹	0	288	9386	0	336	200	100	³⁰
POPE	Slipids ²⁹	0	336	?	0	310	2×200	2×100	³¹
POPE	Slipids ²⁹	0	500	25000	0	310	500	100	³²
POPE	Slipids / Åqvist ^{29,33}	0.11	500	25000	50	310	500	100	³⁴
DPPE	GROMOS-CKP [?]	0	128	3655	0	342	2×500	2×400	³⁵
POPE	GROMOS-CKP [?]	0	128	3552	0	313	2×500	2×400	³⁶
POPE	GROMOS-CKP [?]	0	500	25000	0	310	500	100	³⁷
POPE	GROMOS-CKP [?]	0.11	500	25000	50	310	500	100	³⁸
DOPE	GROMOS-CKP [?]	0	128	4789	0	271	2×500	2×400	³⁹
POPE	GROMOS 43A1-S3 [?]	0	128	3552	0	313	2×200	2×100	⁴⁰
POPE	OPLS-UA vdW on H [?]	0	128	3328	0	303	2×200	2×100	⁴¹
POPE	OPLS-UA [?]	0	128	3328	0	303	2×200	2×100	⁴²
POPE	OPLS-MacRog ⁴³	0	144	5760	0	310	500	350	⁴⁴
POPE	OPLS-MacRog ⁴³	0	128	5120	0	300	500	300	⁴⁵
POPE	Berger-Vries [?]	0	128	3552	0	303	2×200	2×100	⁴⁶
POPE	Berger-largeH [?]	0	128	3552	0	303	2×200	2×100	⁴⁷
DOPE	Berger-Vries [?]	0	128	4789	0	271	2×200	2×100	⁴⁸
DOPE	Berger-largeH [?]	0	128	4789	0	271	2×300	2×100	⁴⁹
POPE	LIPID17 ⁵⁰	0	500	25000	50	310	500	100	⁵¹
POPE	LIPID17 ⁵⁰	0.11	500	25000	50	310	500	100	⁵²

^aNumber of lipid molecules with largest mole fraction

^bNumber of water molecules

^cNumber of additional cations

^dSimulation temperature

^eTotal simulation time

^fTime used for analysis

^gReference for simulation files

3.Citation for CHARMM36ua?

4.Which ion model is used in²⁷?

5.Citation for GROMOS-CKP?

6.Citation for GROMOS 43A1-S3?

7.Citation for OPLS-UA models?

8.Citations for Berger-* simulations?

Table S2: List of MD simulations with PG lipids.

lipid/counter-ions	force field for lipids / ions	NaCl (M)	^a N _l	^b N _w	^c N _c	^d T (K)	^e t _{sim} (ns)	^f t _{anal} (ns)	^g files
POPG/K ⁺	CHARMM36 ⁵³	0	118	4110	0	298	100	100	⁵⁴
POPG	CHARMM36 ⁵³	0.11	500	25000	49	310	500	100	⁵⁵
POPG	CHARMM36 ⁵³	0	500	25000	0	310	500	100	⁵⁶
POPG/Na ⁺	Slipids / Åqvist ^{33,57}	0	288	10664	0	298	250	100	⁵⁸
DPPG/Na ⁺	Slipids / Åqvist ^{33,57}	0	288	11232	0	314	200	100	⁵⁹
DPPG/Na ⁺	Slipids / Åqvist ^{33,57}	0	288	11232	0	298	400	100	⁶⁰
POPG	Slipids / Åqvist ^{33,57}	0	500	25000	0	310	500	100	⁶¹
POPG	Slipids / Åqvist ^{33,57}	0.11	500	25000	49	310	500	100	⁶²
POPG	LIPID17 / Dang ^{50,63,64}	0	500	25000	0	310	500	100	⁶⁵
POPG	LIPID17 ⁵⁰	0.11	500	25000	49	310	500	100	⁶⁶
POPG	GROMOS-CKP [?]	0	500	25000	0	310	500	100	⁶⁷
POPG	GROMOS-CKP [?]	0.11	500	25000	49	310	500	100	⁶⁸

^aNumber of lipid molecules with largest mole fraction

^bNumber of water molecules

^cNumber of additional cations

^dSimulation temperature

^eTotal simulation time

^fTime used for analysis

^gReference for simulation files

9.Citation and ion model for GROMOS-CKP?

Table S3: List of MD simulations with PE and PG lipids mixed with PC.

lipid/counter-ions	force field for lipids / ions	NaCl (M)	CaCl ₂ (M)	^a N _l	^b N _w	^c N _c	^d T (K)	^e t _{sim} (ns)	^f t _{anal} (ns)	^g files
POPC	CHARMM36 ²⁴	0	0	500	25000	0	310	500	100	⁶⁹
POPC:POPG (7:3)	CHARMM36 ^{24,53}	0	0	350	25000	0	310	500	100	⁷⁰
POPC:POPG (1:1)	CHARMM36 ^{24,53}	0	0	150:150	31500	0	298	500	400	⁷¹
POPC:POPG (1:1)	CHARMM36 ^{24,53}	0	0.1	150:150	31329	57	298	400	300	⁷²
POPC:POPG (1:1)	CHARMM36 ^{24,53}	0	1.08	150:150	29766	578	298	500	400	⁷³
POPC:POPG (4:1)	CHARMM36 ^{24,53}	0	0	350:88	26280	0	298	500	400	⁷⁴
POPC:POPG (4:1)	CHARMM36 ^{24,53}	0	0.1	350:88	26280	47	298	500	400	⁷⁵
POPC:POPG (4:1)	CHARMM36 ^{24,53}	0	1.0	350:88	24927	451	298	500	400	⁷⁶
POPC	CHARMM36 ²⁴	0	0	256	8704	0	300	300	250	⁷⁷
POPC:POPE (1:1)	CHARMM36 ^{24,53}	0	0	128	8704	0	300	300	250	⁷⁸
POPC	OPLS-MacRog ⁴³	0	0	128	5120	0	300	500	300	⁷⁹
POPC:POPE (1:1)	OPLS-MacRog ⁴³	0	0	128	5120	0	300	500	300	⁸⁰
POPC	Slipid ²⁹	0	0	512	23943	0	298	170	100	⁸¹
POPC:POPE (1:1)	Slipid ²⁹	0	0	128	5120	0	298	500	300	⁸²
POPC	GROMOS-CKP / ?? [?] ?	0	0	500	25000	0	310	500	100	⁸³
POPC:POPG (7:3)	GROMOS-CKP / ?? [?] ?	0	0	350:150	25000	0	310	500	100	⁸⁴
POPC	Slipid ²⁹	0	0	500	25000	0	310	500	100	⁸⁵
POPC:POPG (7:3)	Slipid / Åqvist ^{29,33}	0	0	350:150	25000	0	310	500	100	⁸⁶
POPC:POPG (1:1)	Slipid / Dang ^{29,63,64,87}	0	0	128:128	12800	0	298	500	400	⁸⁸
POPC:POPG (1:1)	Slipid / Dang ^{29,63,64,87}	0	0.1	128:128	12800	23	298	500	400	⁸⁸
POPC:POPG (1:1)	Slipid / Dang ^{29,63,64,87}	0	0.2	128:128	12800	46	298	1500	500	⁸⁸
POPC:POPG (1:1)	Slipid / Dang ^{29,63,64,87}	0	0.5	128:128	12800	115	298	1500	500	⁸⁸
POPC:POPG (1:1)	Slipid / Dang ^{29,63,64,87}	0	1.0	128:128	12800	230	298	1500	500	⁸⁸

^aNumber of lipid molecules with largest mole fraction

^bNumber of water molecules

^cNumber of additional cations

^dSimulation temperature

^eTotal simulation time

^fTime used for analysis

^gReference for simulation files

10.Citation and ion model for GROMOS-CKP?

Table S4: List of MD simulations with PE and PG lipids mixed with PC.

lipid/counter-ions	force field for lipids / ions	NaCl (M)	CaCl ₂ (M)	^a N _l	^b N _w	^c N _c	^d T (K)	^e t _{sim} (ns)	^f t _{anal} (ns)	^g files
POPC:POPG (4:1)	Lipid17 / Dang ^{50,63,64}	0	0	350:88	26265	0	298	400	350	⁸⁹
POPC:POPG (4:1)	Lipid17 / Dang ^{50,63,64}	0	0.1	350:88	26124	47	298	400	250	⁹⁰
POPC:POPG (4:1)	Lipid17 / Dang ^{50,63,64}	0	1.0	350:88	24840	475	298	1200	200	⁹¹
POPC:POPG (1:1)	Lipid17 / Dang ^{50,63,64}	0	0	150:150	31572	0	298	320	200	⁹²
POPC:POPG (1:1)	Lipid17 / Dang ^{50,63,64}	0	0.1	150:150	31401	57	298	718	198	⁹³
POPC:POPG (1:1)	Lipid17 / Dang ^{50,63,64}	0	1.0	150:150	29865	569	298	720	200	⁹⁴
POPC:POPG (4:1)	Lipid17ecc / ECC-ions ⁹⁵⁻⁹⁷	0	0	350:88	26265	0	298	400	300	⁹⁸
POPC:POPG (4:1)	Lipid17ecc / ECC-ions ⁹⁵⁻⁹⁷	0	0.1	350:88	26124	47	298	400	300	⁹⁹
POPC:POPG (4:1)	Lipid17ecc / ECC-ions ⁹⁵⁻⁹⁷	0	1.0	350:88	24840	475	298	400	300	¹⁰⁰
POPC:POPG (1:1)	Lipid17ecc / ECC-ions ⁹⁵⁻⁹⁷	0	0	150:150	31572	0	298	347.8	333	¹⁰¹
POPC:POPG (1:1)	Lipid17ecc / ECC-ions ⁹⁵⁻⁹⁷	0	0.1	150:150	29865	54	298	400	300	¹⁰²
POPC:POPG (1:1)	Lipid17ecc / ECC-ions ⁹⁵⁻⁹⁷	0	1.0	150:150	29865	569	298	600	400	¹⁰³
POPC	Berger [?] 11.	0	0	256	10240	0	300	300	200	¹⁰⁴
POPC:POPE (1:1)	Berger [?] 12.	0	0	128	11008	0	300	300	200	¹⁰⁵
POPC:DOPE (1:1)	Berger [?] 13.	0	0	128	10240	0	300	300	200	¹⁰⁶
DOPC	Berger [?] 14.	0	0	256	11008	0	300	300	200	¹⁰⁷
DOPC:DOPE (1:1)	Berger [?] 15.	0	0	128	11008	0	300	300	200	¹⁰⁸

^aNumber of lipid molecules with largest mole fraction

^bNumber of water molecules

^cNumber of additional cations

^dSimulation temperature

^eTotal simulation time

^fTime used for analysis

^gReference for simulation files

16.Citation and description for "Berger" model?

References

- (1) Botan, A.; Favela-Rosales, F.; Fuchs, P. F. J.; Javanainen, M.; Kanduč, M.; Kulig, W.; Lamberg, A.; Loison, C.; Lyubartsev, A.; Miettinen, M. S. et al. Toward Atomistic Resolution Structure of Phosphatidylcholine Headgroup and Glycerol Backbone at Different Ambient Conditions. *J. Phys. Chem. B* **2015**, *119*, 15075–15088.
- (2) Antila, H. S.; Buslaev, P.; Favela-Rosales, F.; Mendes Ferreira, T.; Gushchin, I.; Javanainen, M.; Kav, B.; Madsen, J. J.; Melcr, J.; Miettinen, M. S. et al. Headgroup Structure and Cation Binding in Phosphatidylserine Lipid Bilayers. *The Journal of Physical Chemistry B* **2019**, acs.jpcc.9b06091.
- (3) Wohlgemuth, R.; Waespe-Sarcevic, N.; Seelig, J. Bilayers of phosphatidylglycerol. A deuterium and phosphorus nuclear magnetic resonance study of the head-group region. *Biochemistry* **1980**, *19*, 3315–3321.
- (4) Seelig, J.; Gally, H. U. Investigation of phosphatidylethanolamine bilayers by deuterium and phosphorus-31 nuclear magnetic resonance. *Biochemistry* **1976**, *15*, 5199–5204.
- (5) Gally, H. U.; Pluschke, G.; Overath, P.; Seelig, J. Structure of Escherichia coli membranes. Glycerol auxotrophs as a tool for the analysis of the phospholipid head-group region by deuterium magnetic resonance. *Biochemistry* **1981**, *20*, 1826–1831.
- (6) Borle, F.; Seelig, J. Ca²⁺ binding to phosphatidylglycerol bilayers as studied by differential scanning calorimetry and ²H- and ³¹P-nuclear magnetic resonance. *Chemistry and Physics of Lipids* **1985**, *36*, 263 – 283.
- (7) Scherer, P.; Seelig, J. Structure and dynamics of the phosphatidylcholine and the phosphatidylethanolamine head group in L-M fibroblasts as studied by deuterium nuclear magnetic resonance. *EMBO J.* **1987**, *6*.

- (8) Macdonald, P. M.; Seelig, J. Calcium binding to mixed phosphatidylglycerol-phosphatidylcholine bilayers as studied by deuterium nuclear magnetic resonance. *Biochemistry* **1987**, *26*, 1231–1240.
- (9) Ollila, O. S.; Pabst, G. Atomistic resolution structure and dynamics of lipid bilayers in simulations and experiments. *Biochimica et Biophysica Acta (BBA) - Biomembranes* **2016**, *1858*, 2512 – 2528.
- (10) Seelig, J.; MacDonald, P. M.; Scherer, P. G. Phospholipid head groups as sensors of electric charge in membranes. *Biochemistry* **1987**, *26*, 7535–7541.
- (11) Antila, H. S.; Buslaev, P.; Favela-Rosales, F.; Mendes Ferreira, T.; Gushchin, I.; Javanainen, M.; Kav, B.; Madsen, J. J.; Melcr, J.; Miettinen, M. S. et al. Headgroup Structure and Cation Binding in Phosphatidylserine Lipid Bilayers. *The Journal of Physical Chemistry B* **0**, *0*, null.
- (12) Catte, A.; Girych, M.; Javanainen, M.; Loison, C.; Melcr, J.; Miettinen, M. S.; Monticelli, L.; Maatta, J.; Oganessian, V. S.; Ollila, O. H. S. et al. Molecular electrometer and binding of cations to phospholipid bilayers. *Phys. Chem. Chem. Phys.* **2016**, *18*, 32560–32569.
- (13) Melcr, J.; Martinez-Seara, H.; Nencini, R.; Kolafa, J.; Jungwirth, P.; Ollila, O. H. S. Accurate Binding of Sodium and Calcium to a POPC Bilayer by Effective Inclusion of Electronic Polarization. *The Journal of Physical Chemistry B* **2018**, *122*, 4546–4557.
- (14) Melcr, J.; Ferreira, T. M.; Jungwirth, P.; Ollila, O. H. S. Improved Cation Binding to Lipid Bilayers with Negatively Charged POPS by Effective Inclusion of Electronic Polarization. *Journal of Chemical Theory and Computation* **2020**, *16*, 738–748.
- (15) Akutsu, H.; Seelig, J. Interaction of metal ions with phosphatidylcholine bilayer membranes. *Biochemistry* **1981**, *20*, 7366–7373.

- (16) Michaud-Agrawal, N.; Denning, E. J.; Woolf, T. B.; Beckstein, O. MDAnalysis: A toolkit for the analysis of molecular dynamics simulations. *Journal of Computational Chemistry* **2011**, *32*, 2319–2327.
- (17) Richard J. Gowers;; Max Linke;; Jonathan Barnoud;; Tyler J. E. Reddy;; Manuel N. Melo;; Sean L. Seyler;; Jan DomaÅŹski;; David L. Dotson;; SÅľbastien Buchoux;; Ian M. Kenney, et al. MDAnalysis: A Python Package for the Rapid Analysis of Molecular Dynamics Simulations. Proceedings of the 15th Python in Science Conference. 2016; pp 98 – 105.
- (18) McGibbon, R. T.; Beauchamp, K. A.; Harrigan, M. P.; Klein, C.; Swails, J. M.; Hernandez, C. X.; Schwantes, C. R.; Wang, L.-P.; Lane, T. J.; Pande, V. S. MDTraj: A Modern Open Library for the Analysis of Molecular Dynamics Trajectories. *Biophysical Journal* **2015**, *109*, 1528 – 1532.
- (19) Abraham, M.; van der Spoel, D.; Lindahl, E.; Hess, B.; the GROMACS development team, GROMACS user manual version 5.0.7. 2015.
- (20) project, N. NMRLipidsIVb GitHub repository. <https://github.com/NMRLipids/NMRLipidsIVPEandPG>.
- (21) ohsOllila;; et al., MATCH GitHub repository. <https://github.com/NMRLipids/MATCH>.
- (22) Fuchs, P.; et al., BuildH GitHub repository. <https://github.com/patrickfuchs/buildH>.
- (23) Piggot, T. J.; Allison, J. R.; Sessions, R. B.; Essex, J. W. On the Calculation of Acyl Chain Order Parameters from Lipid Simulations. *J. Chem. Theory Comput.* **2017**, *13*, 5683–5696.

- (24) Klauda, J. B.; Venable, R. M.; Freites, J. A.; O'Connor, J. W.; Tobias, D. J.; Mondragon-Ramirez, C.; Vorobyov, I.; MacKerell Jr, A. D.; Pastor, R. W. Update of the CHARMM All-Atom Additive Force Field for Lipids: Validation on Six Lipid Types. *J. Phys. Chem. B* **2010**, *114*, 7830–7843.
- (25) Javanainen, M. Simulation of a POPE bilayer at 310K with the CHARMM36 force field. 2019; <https://doi.org/10.5281/zenodo.2641987>.
- (26) PEON, CHARMM36 POPE Bilayer Simulation (Last 100 ns, 310 K). 2019; <https://doi.org/10.5281/zenodo.3237461>.
- (27) PEÅŞN, A. CHARMM36 POPE Bilayer Simulation (Last 100 ns, 150 mM NaCl, 310 K). 2019; <https://doi.org/10.5281/zenodo.2577454>.
- (28) Piggot, T. CHARMM36-UA POPE Simulations (versions 1 and 2) 310 K (NOTE: hexagonal membrane and POPE is called PEUA). 2018; <https://doi.org/10.5281/zenodo.1293774>.
- (29) Jämbeck, J. P. M.; Lyubartsev, A. P. An Extension and Further Validation of an All-Atomistic Force Field for Biological Membranes. *J. Chem. Theory Comput.* **2012**, *8*, 2938–2948.
- (30) Favela-Rosales, F. MD simulation trajectory of a fully hydrated DPPE bilayer: SLIPIDS, Gromacs 5.0.4. 2017. 2017; <https://doi.org/10.5281/zenodo.495247>.
- (31) Piggot, T. Slipids POPE Simulations (versions 1 and 2) 310 K (NOTE: hexagonal membrane). 2018; <https://doi.org/10.5281/zenodo.1293813>.
- (32) Peon, A. SLIPID POPE Bilayer Simulation (Last 100 ns, 310 K). 2019; <https://doi.org/10.5281/zenodo.3231342>.
- (33) Åqvist, J. Ion-water interaction potentials derived from free energy perturbation simulations. *J. Phys. Chem.* **1990**, *94*, 8021–8024.

- (34) PEÅŞN, A. SLIPID POPE Bilayer Simulation (Last 100 ns, 150 mM NaCl, 310 K). 2019; <https://doi.org/10.5281/zenodo.2578069>.
- (35) Piggot, T. GROMOS-CKP DPPE Simulations (versions 1 and 2) 342 K. 2018; <https://doi.org/10.5281/zenodo.1293957>.
- (36) Piggot, T. GROMOS-CKP POPE Simulations (versions 1 and 2) 313 K. 2018; <https://doi.org/10.5281/zenodo.1293932>.
- (37) PEON, A. GROMOS POPE Bilayer Simulation (Last 100 ns, 310 K). 2019; <https://doi.org/10.5281/zenodo.3237754>.
- (38) PEÅŞN, A. Gromos POPE Bilayer Simulation (Last 100 ns, 150 mM NaCl, 310 K). 2019; <https://doi.org/10.5281/zenodo.2574491>.
- (39) Piggot, T. GROMOS-CKP DOPE Simulations (versions 1 and 2) 271 K. 2018; <https://doi.org/10.5281/zenodo.1293941>.
- (40) Piggot, T. GROMOS 43A1-S3 POPE Simulations (versions 1 and 2) 313 K (NOTE: anisotropic pressure coupling). 2018; <https://doi.org/10.5281/zenodo.1293762>.
- (41) Piggot, T. OPLS-UA POPE Simulations (versions 1 and 2) 303 K with vdW on H atoms. 2018; <https://doi.org/10.5281/zenodo.1293853>.
- (42) Piggot, T. OPLS-UA POPE Simulations (versions 1 and 2) 303 K. 2018; <https://doi.org/10.5281/zenodo.1293855>.
- (43) RÅsg, T.; OrÅĆowski, A.; Llorente, A.; Skotland, T.; SylvÅdnne, T.; Kauhanen, D.; Ekroos, K.; Sandvig, K.; Vattulainen, I. Data including GROMACS input files for atomistic molecular dynamics simulations of mixed, asymmetric bilayers including molecular topologies, equilibrated structures, and force field for lipids compatible with OPLS-AA parameters. *Data in Brief* **2016**, 7, 1171 – 1174.

- (44) Javanainen, M. Simulation of a POPE bilayer, lipid model based on OPLS-aa by Rog et al. 2019; <https://doi.org/10.5281/zenodo.3571071>.
- (45) Milan Rodriguez, P.; Fuchs, P. F. MacRog pure POPE MD simulation (300 K - 500ns - 1 bar). 2020; <https://doi.org/10.5281/zenodo.3725670>.
- (46) Piggot, T. Berger POPE Simulations (versions 1 and 2) 303 K - de Vries repulsive H. 2018; <https://doi.org/10.5281/zenodo.1293889>.
- (47) Piggot, T. Berger POPE Simulations (versions 1 and 2) 303 K - larger repulsive H. 2018; <https://doi.org/10.5281/zenodo.1293891>.
- (48) Piggot, T. Berger DOPE Simulations (versions 1 and 2) 271 K - de Vries repulsive H. 2018; <https://doi.org/10.5281/zenodo.1293928>.
- (49) Piggot, T. Berger DOPE Simulations (versions 1 and 2) 271 K - larger repulsive H. 2018; <https://doi.org/10.5281/zenodo.1293905>.
- (50) Gould, I.; Skjevik, A.; Dickson, C.; Madej, B.; Walker, R. Lipid17: A Comprehensive AMBER Force Field for the Simulation of Zwitterionic and Anionic Lipids. 2018; In preparation.
- (51) PEON, A. LIPID17 POPE Bilayer Simulation (Last 100 ns, 310 K) using dihedral 9. 2019; <https://doi.org/10.5281/zenodo.4424292>.
- (52) PEÅŞN, A. LIPID17 POPE Bilayer Simulation (Last 100 ns, 150 mM NaCl, 310 K) using dihedral 9. 2019; <https://doi.org/10.5281/zenodo.4424934>.
- (53) Venable, R. M.; Luo, Y.; Gawrisch, K.; Roux, B.; Pastor, R. W. Simulations of Anionic Lipid Membranes: Development of Interaction-Specific Ion Parameters and Validation Using NMR Data. *The Journal of Physical Chemistry B* **2013**, *117*, 10183–10192.

- (54) Ollila, O. H. S. POPG lipid bilayer simulation at T298K ran with MODEL_CHARMM_GUI force field and Gromacs. 2017; <https://doi.org/10.5281/zenodo.1011096>.
- (55) PEÄŞN, A. CHARMM36 POPG Bilayer Simulation (Last 100 ns, 150 mM NaCl, 310 K). 2019; <https://doi.org/10.5281/zenodo.2573531>.
- (56) ANTONIO, CHARMM36 POPG Bilayer Simulation (Last 100 ns, 310 K). 2019; <https://doi.org/10.5281/zenodo.3237463>.
- (57) Jämbeck, J. P. M.; Lyubartsev, A. P. Implicit inclusion of atomic polarization in modeling of partitioning between water and lipid bilayers. *Phys. Chem. Chem. Phys.* **2013**, *15*, 4677–4686.
- (58) Favela-Rosales, F. MD simulation trajectory of a fully hydrated POPG bilayer: SLIPIDS, Gromacs 5.0.4. 2017. 2017; <https://doi.org/10.5281/zenodo.546133>.
- (59) Favela-Rosales, F. MD simulation trajectory of a fully hydrated DPPG bilayer @314K: SLIPIDS, Gromacs 5.0.4. 2017. 2017; <https://doi.org/10.5281/zenodo.546136>.
- (60) Favela-Rosales, F. MD simulation trajectory of a fully hydrated DPPG bilayer @298K: SLIPIDS, Gromacs 5.0.4. 2017. 2017; <https://doi.org/10.5281/zenodo.546135>.
- (61) PeÄşn, A. LIPID17 POPG Bilayer Simulation (Last 100 ns, 310 K) using dihedral type 9. 2019; <https://doi.org/10.5281/zenodo.3832274>.
- (62) PEÄŞN, A. SLIPID POPG Bilayer Simulation (Last 100 ns, 150 mM NaCl, 310 K). 2019; <https://doi.org/10.5281/zenodo.2633773>.
- (63) Smith, D. E.; Dang, L. X. Computer simulations of NaCl association in polarizable water. *J. Chem. Phys* **1994**, *100*, 3757–3766.

- (64) Dang, L. X.; Schenter, G. K.; Glezakou, V.-A.; Fulton, J. L. Molecular simulation analysis and X-ray absorption measurement of Ca^{2+} , K^{+} and Cl^{-} ions in solution. *J. Phys. Chem. B* **2006**, *110*, 23644–54.
- (65) PeÅşn, A. LIPID17 POPG Bilayer Simulation (Last 100ns, 310 K) using dihedral type 9 instead of type 1. 2020; <https://doi.org/10.5281/zenodo.3832219>.
- (66) PEÅŞN, A. LIPID17 POPG Bilayer Simulation (Last 100 ns, 150 mM NaCl, 310 K) using dihedral type 9. 2019; <https://doi.org/10.5281/zenodo.4386514>.
- (67) PEON, A. GROMOS POPG Bilayer Simulation (Last 100 ns, 310 K). 2019; <https://doi.org/10.5281/zenodo.3266166>.
- (68) PEÅŞN, A. Gromos POPG Bilayer Simulation (Last 100 ns, 150 mM NaCl, 310 K). 2019; <https://doi.org/10.5281/zenodo.3257649>.
- (69) PEON, A. CHARMM36 POPC Bilayer Simulation (Last 100 ns, 310 K). 2019; <https://doi.org/10.5281/zenodo.3247813>.
- (70) PEON, A. CHARMM36 POPC-POPG 7:3 Bilayer Simulation (Last 100 ns, 310 K). 2019; <https://doi.org/10.5281/zenodo.3248689>.
- (71) Kiirikki, A. M.; Ollila, O. H. S. POPC:POPG 1:1 MD simulation with CHARMM36 in water and Na^{+} counter ions. 2020; <https://doi.org/10.5281/zenodo.3997116>.
- (72) Kiirikki, A. M.; Ollila, O. H. S. POPC:POPG 1:1 MD simulation with CHARMM36 in 0.1 M CaCL solution and Na^{+} counter ions. 2020; <https://doi.org/10.5281/zenodo.4005515>.
- (73) Kiirikki, A. M.; Ollila, O. H. S. POPC:POPG 1:1 MD simulation with CHARMM36 in 1 M CaCL solution and Na^{+} counter ions. 2020; <https://doi.org/10.5281/zenodo.3997135>.

- (74) Kiirikki, A. M.; Ollila, O. H. S. POPC:POPG 4:1 MD simulation with CHARMM36 in water with Na⁺ counter ions. 2020; <https://doi.org/10.5281/zenodo.3996952>.
- (75) Kiirikki, A. M.; Ollila, O. H. S. POPC:POPG 4:1 MD simulation with CHARMM36 in 0.1 M CaCl₂ solution with Na⁺ counter ions. 2020; <https://doi.org/10.5281/zenodo.3997019>.
- (76) Kiirikki, A. M.; Ollila, O. H. S. POPC:POPG 4:1 MD simulation with CHARMM36 in 1 M CaCl₂ solution with Na⁺ counterions. 2020; <https://doi.org/10.5281/zenodo.3997037>.
- (77) Papadopoulos, C.; Fuchs, P. F. CHARMM36 pure POPC MD simulation (300 K - 300ns - 1 bar). 2018; <https://doi.org/10.5281/zenodo.1306800>.
- (78) Papadopoulos, C.; Fuchs, P. F. CHARMM36 POPC/POPE (50%-50%) MD simulation (300 K - 300ns - 1 bar). 2018; <https://doi.org/10.5281/zenodo.1306821>.
- (79) Milan Rodriguez, P.; Fuchs, P. F. MacRog pure POPC MD simulation (300 K - 500ns - 1 bar). 2020; <https://doi.org/10.5281/zenodo.3741793>.
- (80) Milan Rodriguez, P.; Fuchs, P. F. MacRog POPC/POPE 1:1 MD simulation (300 K - 500ns - 1 bar). 2020; <https://doi.org/10.5281/zenodo.3725637>.
- (81) Favela-Rosales, F. MD simulation trajectory of a lipid bilayer: Pure POPC in water. SLIPIDS, Gromacs 4.6.3. 2016. 2016; <https://doi.org/10.5281/zenodo.166034>.
- (82) Javanainen, M. Simulation of POPC:POPE 1:1 membrane with the Slipids force field. 2020; <https://doi.org/10.5281/zenodo.3605386>.
- (83) PEON, A. GROMOS-CKP POPC Bilayer Simulation (Last 100 ns, 310 K). 2019; <https://doi.org/10.5281/zenodo.3247435>.
- (84) PEON, A. GROMOS-CKP POPC-POPG 7:3 Bilayer Simulation (Last 100 ns, 310 K). 2019; <https://doi.org/10.5281/zenodo.3266240>.

- (85) PEON, A. SLIPID POPC Bilayer Simulation (Last 100 ns, 310 K). 2019; <https://doi.org/10.5281/zenodo.3235552>.
- (86) PeON, A. SLIPID POPC-POPG 7:3 Bilayer Simulation (Last 100 ns, 310 K). 2019; <https://doi.org/10.5281/zenodo.3240156>.
- (87) Jämbeck, J. P.; Lyubartsev, A. P. Another piece of the membrane puzzle: extending slipids further. *Journal of chemical theory and computation* **2012**, *9*, 774–784.
- (88) Javanainen, M. Simulations of POPC:POPG 1:1 membranes with varying levels of CaCl₂ using the Slipids force field. 2020; <https://doi.org/10.5281/zenodo.3613573>.
- (89) Virtanen, S.; Ollila, O. H. S. LIPID17 POPC-POPG 80:20 MD simulation, Na⁺ counterions, 298K. 2019; <https://doi.org/10.5281/zenodo.3693681>.
- (90) Virtanen, S.; Ollila, O. H. S. LIPID17 POPC-POPG 80:20 MD simulation, Na⁺ counterions and 100mM CaCl₂, 298K. 2019; <https://doi.org/10.5281/zenodo.3833725>.
- (91) Virtanen, S.; Ollila, O. H. S. LIPID17 POPC-POPG 80:20 MD simulation, Na⁺ counterions and 1000mM CaCl₂, 298K. 2019; <https://doi.org/10.5281/zenodo.3874378>.
- (92) Virtanen, S.; Ollila, O. H. S. LIPID17 POPC-POPG 50:50 MD simulation, Na⁺ counterions, 298K. 2019; <https://doi.org/10.5281/zenodo.3857816>.
- (93) Virtanen, S.; Ollila, O. H. S. LIPID17 POPC-POPG 50:50 MD simulation, Na⁺ counterions and 100mM CaCl₂, 298K. 2019; <https://doi.org/10.5281/zenodo.3871590>.
- (94) Virtanen, S.; Ollila, O. H. S. LIPID17 POPC-POPG 50:50 MD simulation, Na⁺ counterions and 1000mM CaCl₂, 298K. 2019; <https://doi.org/10.5281/zenodo.3864993>.

- (95) Pluhařová, E.; Fischer, H. E.; Mason, P. E.; Jungwirth, P. Hydration of the chloride ion in concentrated aqueous solutions using neutron scattering and molecular dynamics. *Mol. Phys.* **2014**, *112*, 1230–1240.
- (96) Kohagen, M.; Mason, P. E.; Jungwirth, P. Accounting for Electronic Polarization Effects in Aqueous Sodium Chloride via Molecular Dynamics Aided by Neutron Scattering. *J. Phys. Chem. B* **2016**, *120*, 1454–1460.
- (97) Martínek, T.; Duboué-Dijon, E.; Timr, Š.; Mason, P. E.; Baxová, K.; Fischer, H. E.; Schmidt, B.; Pluhařová, E.; Jungwirth, P. Calcium ions in aqueous solutions: Accurate force field description aided by ab initio molecular dynamics and neutron scattering. *J. Chem. Phys.* **2018**, *148*, 222813.
- (98) Kiirikki, A. M.; Ollila, O. H. S. Lipid17ecc POPC:POPG 4:1 MD simulation in water with Na⁺ counter ions. 2020; <https://doi.org/10.5281/zenodo.3997154>.
- (99) Kiirikki, A. M.; Ollila, O. H. S. Lipid17ecc POPC:POPG 4:1 bilayer simulation in 0.1 M CaCl₂ solution and Na⁺ counter ions. 2020; <https://doi.org/10.5281/zenodo.3997176>.
- (100) Kiirikki, A. M.; Ollila, O. H. S. Lipid17ecc POPC:POPG 4:1 bilayer simulation in 1 M CaCl₂ solution and Na⁺ counter ions. 2020; <https://doi.org/10.5281/zenodo.4492639>.
- (101) Ollila, O. H. S.; Virtanen, I. S. ECC-LIPID17 POPC-POPG 50:50 MD simulation, Na⁺ counterions, 298K. 2020; <https://doi.org/10.5281/zenodo.3859339>.
- (102) Ollila, O. H. S.; Virtanen, I. S. ECC-LIPID17 POPC-POPG 50:50 MD simulation, Na⁺ counterions and 100mM CaCl₂, 298K. 2020; <https://doi.org/10.5281/zenodo.3855729>.

- (103) Ollila, O. H. S.; Virtanen, I. S. ECC-LIPID17 POPC-POPG 50:50 MD simulation, Na⁺ counterions and 1000mM CaCl₂, 298K. 2020; <https://doi.org/10.5281/zenodo.3862036>.
- (104) AmÄllie, B.; F.J., F. P. Berger pure POPC MD simulation (300 K - 300ns - 1 bar). 2018; <https://doi.org/10.5281/zenodo.1402417>.
- (105) AmÄllie, B.; F.J., F. P. Berger POPC/POPE (50:50 ratio) MD simulation (300 K - 400ns - 1 bar). 2018; <https://doi.org/10.5281/zenodo.1402449>.
- (106) AmÄllie, B.; F.J., F. P. Berger POPC/DOPE (50:50 ratio) MD simulation (300 K - 300ns - 1 bar). 2018; <https://doi.org/10.5281/zenodo.1402441>.
- (107) AmÄllie, B.; F.J., F. P. Berger pure DOPC MD simulation (300 K - 300ns - 1 bar). 2018; <https://doi.org/10.5281/zenodo.1402411>.
- (108) AmÄllie, B.; F.J., F. P. Berger DOPC/DOPE (50:50 ratio) MD simulation (300 K - 300ns - 1 bar). 2018; <https://doi.org/10.5281/zenodo.1402437>.
- (109) Lee, J.; Cheng, X.; Swails, J. M.; Yeom, M. S.; Eastman, P. K.; Lemkul, J. A.; Wei, S.; Buckner, J.; Jeong, J. C.; Qi, Y. et al. CHARMM-GUI Input Generator for NAMD, GROMACS, AMBER, OpenMM, and CHARMM/OpenMM Simulations Using the CHARMM36 Additive Force Field. *Journal of Chemical Theory and Computation* **2016**, *12*, 405–413.
- (110) Nose, S. A molecular dynamics method for simulations in the canonical ensemble. *Mol. Phys.* **1984**, *52*, 255–268.
- (111) Hoover, W. G. Canonical dynamics: Equilibrium phase-space distributions. *Phys. Rev. A* **1985**, *31*, 1695–1697.
- (112) Parrinello, M.; Rahman, A. Polymorphic transitions in single crystals: A new molecular dynamics method. *J. Appl. Phys.* **1981**, *52*, 7182–7190.

- (113) Páll, S.; Zhmurov, A.; Bauer, P.; Abraham, M.; Lundborg, M.; Gray, A.; Hess, B.; Lindahl, E. Heterogeneous parallelization and acceleration of molecular dynamics simulations in GROMACS. *The Journal of Chemical Physics* **2020**, *153*, 134110.
- (114) Ghahremanpour, M. M.; Arab, S. S.; Aghazadeh, S. B.; Zhang, J.; van der Spoel, D. MemBuilder: a web-based graphical interface to build heterogeneously mixed membrane bilayers for the GROMACS biomolecular simulation program. *Bioinformatics* **2013**, *30*, 439–441.
- (115) Jorgensen, W. L.; Chandrasekhar, J.; Madura, J. D.; Impey, R. W.; Klein, M. L. Comparison of simple potential functions for simulating liquid water. *J. Chem. Phys.* **1983**, *79*, 926–935.
- (116) Abraham, M. J.; Murtola, T.; Schulz, R.; Páll, S.; Smith, J. C.; Hess, B.; Lindahl, E. GROMACS: High performance molecular simulations through multi-level parallelism from laptops to supercomputers. *SoftwareX* **2015**, *1*, 19–25.
- (117) Darden, T.; York, D.; Pedersen, L. Particle mesh Ewald: An N·log(N) method for Ewald sums in large systems. *J. Chem. Phys.* **1993**, *98*, 10089–10092.
- (118) Essman, U. L.; Perera, M. L.; Berkowitz, M. L.; Larden, T.; Lee, H.; Pedersen, L. G. A smooth particle mesh ewald potential. *J. Chem. Phys.* **1995**, *103*, 8577–8592.
- (119) Hess, B.; Bekker, H.; Berendsen, H. J. C.; Fraaije, J. G. E. M. LINCS: a linear constraint solver for molecular dynamics simulations. *J. Comput. Chem.* **1997**, *18*, 1463–1472.
- (120) Miyamoto, S.; Kollman, P. A. SETTLE: An analytical Version of the SHAKE and RATTLE Algorithm for Rigid Water Models. *J. Comput. Chem* **1992**, *13*, 952–962.
- (121) PEÑÓN, A. LIPID17 POPC-POPG 7:3 Bilayer Simulation (Last 100 ns, 150 mM NaCl, 310 K). 2019; <https://doi.org/10.5281/zenodo.2585523>.

- (122) Páll, S.; Hess, B. A flexible algorithm for calculating pair interactions on {SIMD} architectures. *Comput. Phys. Commun.* **2013**, *184*, 2641 – 2650.
- (123) Bussi, G.; Donadio, D.; Parrinello, M. Canonical sampling through velocity rescaling. *J. Chem. Phys.* **2007**, *126*.
- (124) Dubou  l-Dijon, E.; Javanainen, M.; Delcroix, P.; Jungwirth, P.; Martinez-Seara, H. A practical guide to biologically relevant molecular simulations with charge scaling for electronic polarization. *The Journal of Chemical Physics* **2020**, *153*, 050901.
- (125) Berendsen, H. J. C.; Grigera, J. R.; Straatsma, T. P. The missing term in effective pair potentials. *The Journal of Physical Chemistry* **1987**, *91*, 6269–6271.